*Geology of Ore Deposits, Vol. 45, No. 2, 2003, pp. 151–165. Translated from Geologiya Rudnykh Mestorozhdenii, Vol. 45, No. 2, 2003, pp. 172–187.*


# A Structural–Chemical Approach to Selecting Crystalline Matrices for Actinide Immobilization

**S. V. Yudintsev**[1]

*Institute of Geology of Ore Deposits, Petrography, Mineralogy, and Geochemistry, Russian Academy of Sciences, Staromonetnyi per. 35, Moscow, 119017 Russia*

Received December 19, 2002

**Abstract**—The use of confinement matrices is a key part of safe management of high-level radioactive wastes (HLWs) derived in the nuclear fuel cycle. The matrices should immobilize radioisotopes after HLW deposition in the geological environment with possible groundwater filtration. The glasses currently used for this purpose on an industrial scale are not capable of incorporating sufficient amounts of plutonium and have low stability to chemical corrosion. This paper summarizes the results of structural analysis of crystalline phases that could be used for immobilization of actinide wastes of various compositions. It was suggested that pyrochlore-type phases can be used for incorporation of the actinide–zirconium–rare-earth element fraction of HLWs, while ferrites with a garnet structure could be used for immobilization of wastes of complex composition with high contents of corrosion products (Fe, Al, Ga). Ceramics of such composition were synthesized and analyzed for concentrations of actinides (Th, U), rare-earth elements (Gd, Ce), and Zr. It is necessary to study the stability of these phases to radiation and chemical corrosion to select suitable matrix materials.

## INTRODUCTION

The reprocessing of irradiated fuel of atomic power stations results in the formation of a great amount of radioactive wastes, including high-level radioactive wastes (HLWs). The latter compose only a small part of radioactive wastes by volume, but produce the major part of the total radioactive waste activity. HLWs contain (Table 1) fission products, activated products of corrosion, actinides (including products of nuclear reactions in reactors), and numerous nonradioactive elements, i.e., isotopes of fission products, technological contaminants, etc. (Flowers *et al.*, 1986; Roedder, 1990). Actinides and some long-lived products of their fission ($^{93}$Zr, $^{99}$Tc, $^{126}$Sn, etc.) are the most hazardous radionuclides, which it is proposed to immobilize in secure confinement matrices and deposit at a depth in the Earth's interior (Ringwood, 1985). Selection of suitable immobilizing materials is a key part of safe HLW management in the nuclear fuel cycle. The search for HLW immobilization matrices began in the 1950s with study of various glassy and crystalline materials containing silicates, phosphates, and titanates (*Radioactive Waste …*, 1988). Various glasses are currently used for this purpose on an industrial scale, borosilicate glasses outside Russia and alumophosphate glasses in Russia (Hench *et al.*, 1984; Vashman *et al.*, 1997). However, these glasses are not capable of incorporating sufficient amounts of actinides (particularly, Pu) and have low resistance to chemical corrosion by groundwater (Matzke and van Geel, 1996; Laverov *et al.*, 1997; Matyunin, 2000; Kotova, 2001). The interaction of glass matrices with groundwater results in the formation of colloidal particles (*Glass as a Waste Form …*, 1996), which can carry actinides for long distances. The glasses can crystallize on aging, which decreases the radionuclide stability in the matrix because of formation of soluble phases, such as alkali and alkaline-earth silicates and phosphates, as well as molybdates.

For efficient management of high-level radioactive wastes, they should be separated into several radionuclide fractions (*Actinide and Fission Product Partitioning …*, 1999). One of them contains a few tens of weight percent of actinides and significant amounts of zirconium and lanthanides. The liquid HLWs from reprocessing of the irradiated fuel of various reactors contain (Sombret, 1987) actinides (10–15 wt %), lanthanides (60–65 wt %), and zirconium (20–25 wt %). Among actinides, U, Np, Pu, and Am dominate; among lanthanides, Nd, Ce, La, and Pr. One more group of wastes with high actinide content is produced in conversion of metallic "weapons" plutonium into nuclear fuel (Grachev *et al.*, 2002).

Actinide-rich waste forms alternative to glasses are crystalline matrices (Ringwood, 1985; Vance *et al.*, 1995; Lutze and Ewing, 1995). More than 20 phases have been proposed, differing in their capability for actinide incorporation, as well as in resistance to chemical and radioactive impact (Fielding and White, 1987; *Radioactive Waste …*, 1988; Weber *et al.*, 1998; Yudintsev, 2000). The pyrochlore-type matrix (Ca, Gd, U, Pu, Hf)$_2$Ti$_2$O$_7$ was developed in the United States for immobilization of excess plutonium (Ebbinghaus *et al.*, 1998). Zircon, zirconolite, cubic zirconium dioxide, perovskite, Y–Al garnet, britholite, monazite, and some

[1]Corresponding author: S.V. Yudintsev. E-mail: syud@igem.ru

**Table 1.** Major radioisotopes in high-level radioactive wastes from reprocessing of irradiated nuclear fuel and their half-life periods

| Major fission and corrosion products (β and γ emitters) | | Transuranium actinides (α emitters) | |
|---|---|---|---|
| radionuclide | $T_{1/2}$, year | radionuclide | $T_{1/2}$, year |
| $^{90}Sr$ | 29 | $^{237}Np$ | $2.1 \times 10^6$ |
| $^{93}Zr$ | $1.5 \times 10^6$ | $^{238}Pu$ | 89.9 |
| $^{99}Tc$ | $2.1 \times 10^5$ | $^{239}Pu$ | $2.4 \times 10^4$ |
| $^{126}Sn$ | $10^5$ | $^{240}Pu$ | $6.5 \times 10^3$ |
| $^{129}I$ | $1.7 \times 10^7$ | $^{241}Pu$ | 14 |
| $^{137}Cs$ | 30 | $^{242}Pu$ | $3.78 \times 10^5$ |
| $^{147}Pm$ | 2.6 | $^{241}Am$ | 433 |
| $^{151}Sm$ | 93 | $^{242}Am$ | 152 |
| $^{154}Eu$ | 16 | $^{243}Am$ | $7.3 \times 10^3$ |
| Activated corrosion products | | $^{243}Cm$ | 28 |
| $^{59}Ni$ | $7.5 \times 10^4$ | $^{244}Cm$ | 17.9 |
| $^{60}Co$ | 5.3 | $^{245}Cm$ | $8.5 \times 10^3$ |
| $^{63}Ni$ | 96 | $^{246}Cm$ | $4.76 \times 10^3$ |

other materials have been proposed for immobilization of Pu-bearing wastes (Vance *et al.*, 1995; Burakov *et al.*, 1999, 2000; Ewing, 1999). The search for matrices for actinide immobilization is still an urgent task.

Synthetic materials for immobilization of various radioactive wastes have been studied for about ten years at the Institute of Geology of Ore Deposits, Petrography, Mineralogy, and Geochemistry, Russian Academy of Sciences. This work is being carried out together with scientists from the Radon Scientific Industrial Association, Moscow; the Bochvar All-Russia Research Institute of Inorganic Materials; the Institute of Physics and Power Engineering; the Vernadsky Institute of Geochemistry and Analytical Chemistry, Russian Academy of Sciences; and some other institutions (including some outside Russia). This research is a part of basic principles study aimed at development of a basement for safe HLW disposal, initiated in the early 1990s and supervised by Academician N.P. Laverov.

From a structural perspective, phases stable upon wide variations of waste compositions are preferable. Such phases can be used for immobilization of excess plutonium or compositionally more complex wastes, i.e., actinide–Zr–REE fractions of HLW, actinides and their fission products ($^{93}Zr$, $^{99}Tc$, $^{126}Sn$, etc.), remnants of metallic plutonium converted into nuclear fuel, etc. The search for HLW matrices can be optimized by preliminary analysis of the crystal structures of promising phases. The results of such analysis reduce the amount of potential compounds, which simplifies further experimental examination of the selected materials. The efficiency of such an approach was demonstrated for titanates and aluminates with zirconolite, perovskite, hibonite, and hollandite structures (Fielding and White, 1987). The capabilities of this approach are shown here for matrices with pyrochlore- and garnet-type structures. The results of theoretical analysis helped us to select the most appropriate compounds with the highest capacity to incorporate actinides. These compounds were synthesized and studied by various methods.

## GENERAL INFORMATION ON PYROCHLORE STRUCTURE

The pyrochlore structure ($Fd3m$, $Z = 8$) is a derivative of the fluorite-type structure (Belov, 1950). It can be represented as two fluorite cells sharing a common edge, with half of the coordination polyhedra each lacking two diagonal anions. As a result, the cube is modified to a flattened octahedron and the formula is transformed from $A_4X_8$ (quadruple fluorite formula) into $^{VIII}A_2{}^{VI}B_2{}^{IV}Y_6{}^{IV}X$. $A$ and $B$ are cations in two structural sites, and $Y$ and $X$ are anions, of which $Y$ ($O^{2-}$ anions) are involved in octahedra, while $X$ ($O^{2-}$, $F^-$, $Cl^-$, $OH^-$) are located in interstices and do not participate in the structural framework. The coordination numbers (CN) of ions in this structure can be described by the following codes: $AX_6Y_2$, $BX_6$, $XA_2B_2$, and $YA_4$. The pyrochlore structure can also be represented (Subramanian *et al.*, 1983) as a 3D framework of $B_2O_6$ octahedra sharing common vertices, which includes $[A]^{VIII}$ cations and additional $[X]^{IV}$ anions in the interstices. This is why the hydrothermal alteration of natural pyro-

chlores is accompanied by exchange reactions involving these ions (*Mineraly* …, 1967; Lumpkin *et al.*, 1986).

Natural phases of the pyrochlore group are solid solutions of the composition $[(Na, Ca, REE, U, Th)_2(Nb, Ta, Ti, Zr)_2O_6(F, OH)]$. The actual mineral composition differs from the ideal formula $A_2B_2O_7$ and corresponds to the stoichiometry of the phase $A_{2-m}B_2O_{6-n}X_{1-p}$, where $m$ = 0–1.7, $n$ = 0–0.7, and $p$ = 0–1.0. The A site, with CN = 8, is occupied by cations with charges from +1 to +6 and ionic radii from 0.86 to 1.55 Å. The B site is occupied by cations with charges from +3 to +6 and ionic radii from 0.6 to 0.83 Å. This group comprises the following minerals (according to the cation occupation in the B site): pyrochlore (B = Nb, Ti; Nb + Ta > 2Ti and Nb ≥ Ta), microlite (B = Ta, Ti; Nb + Ta > 2Ti and Ta > Nb), and betafite (B = Nb, Ta, Ti; 2Ti ≥ Nb + Ta). They show a deficiency in atoms in the A site and $O^{2-}$ anions because of isomorphic substitution of high field strength cations ($U^{4+}$, $Th^{4+}$, $REE^{3+}$) in the A site and replacement of oxygen by other anions with a change in the total charge in the anionic part (Lumpkin *et al.*, 1986). There are pyrochlores enriched in U (up to 20 wt %), Th (up to 5 wt %), rare-earth elements (generally LREEs from La to Dy; up to 15 wt %), Sr (up to 6 wt %), Ba (up to 14 wt %), and Pb (up to 40 wt %). The octahedrally coordinated site CN = 6 is occupied by Ti (up to 14 wt %), Zr (up to 6 wt %), and Sn (up to 4 wt %). The radioactive varieties of the mineral are metamict. Heating of the mineral leads to recovering of its crystal structure. The unit cell size of the minerals of the pyrochlore group varies from 10.3 to 10.5 Å and increases up to 10.6 Å with incorporation of large ions of Sr, Ba, and Pb.

The pyrochlore-type structure is typical of many synthetic phases $^{VIII}(A_1A_2)^{VI}(B_1B_2)O_7$, where $A_{1(2)}$ and $B_{1(2)}$ are cations with charges from +1 to +4 and from +3 to +5, respectively (Subramanian *et al.*, 1983; Chakoumakos, 1984). More than 500 various compounds $A_2B_2O_6X$ were synthesized, where A and B are cations with charges from +1 to +4 (in the A site) and from +3 to +5 (in the B site) and X are divalent ($O^{2-}$) and monovalent ($F^-$, $Cl^-$, $Br^-$, $OH^-$) anions. The unit cell sizes vary from 9.3 to 12.0 Å, which is about two times larger than those for phases with the fluorite-type structures. Phases with actinides in all or part of the structural sites were also obtained (Chakoumakos and Ewing, 1985; Ringwood, 1985; Vance *et al.*, 1995; Raison *et al.*, 1999; Laverov *et al.*, 2001). They are of great interest as potential HLW matrices. The features of the pyrochlore-type structures that should be taken into account in selection of phases for immobilization of actinide-bearing HLW are considered below.

## CONDITIONS OF STABILITY OF THE PYROCHLORE STRUCTURE

The structural–chemical features of the pyrochlore-type phases are interrelated (Belov, 1950; McCauley, 1980; Wang *et al.*, 1999, etc.). In addition to the general condition of charge balance, correspondence between cation sizes in the two sites is a very important requirement for stability of the pyrochlore structure. Geometrical analysis shows (Isupov, 1958) that the $(A^{3+})_2(B^{4+})_2O_7$ phases crystallize in the pyrochlore structural type if the ratio $(R_A + R_O) : (R_B + R_O)$ is between 1.08 and 1.22. $R_A$ and $R_B$ denote the radii of ions in the A and B sites, and $R_O$ is the radius of the oxygen anion. For highly polarized ions with CN = 8, e.g., $Bi^{3+}$, the ratio can increase up to 1.33. Similar values are given by Wang *et al.* (1999), who suggested that the $(R_A + R_O) : (R_B + R_O)$ ratio should be between 1.10 and 1.24 for stability of the pyrochlore structure. Therefore, the ratio of cation sizes in the two sites in the pyrochlore structure can vary between 1.3–1.8. A narrower range of 1.46–1.80 is given in by Raison *et al.* (1999) and Begg *et al.* (2001). A change in the ratio beyond this interval leads to destabilization of the pyrochlore structure and the formation of phases with other crystal structures. On the basis of these data, we can determine the elements in the A site with CN = 8 (including actinides) that can associate with various cations in the B site with CN = 6 to form a $(A^{3+})_2(B^{4+})_2O_7$ phase with the pyrochlore structure. For example, for stabilization of titanate pyrochlores ($[B]^{VI} = Ti^{4+}$, $R_{VI}$ = 0.605 Å), the cations in the A site should have radii between 0.8 and 1.0 Å, while larger cations with radii from 0.9 to 1.2 Å are necessary to stabilize the zirconate phases ($R_{VI}$ = 0.72 Å). The stability of phases with pyrochlore structure containing actinides, Zr, REEs, and Hf is estimated below.

## SYNTHESIZED PYROCHLORE-TYPE PHASES WITH REES AND ACTINIDES

Actinides (except for Th, which has a constant valence of +4) can occur in crystal phases in various oxidation states (Begg *et al.*, 1997, 1998). Under conditions of HLW matrix synthesis (1300–1500°C in Ar, Ar + $H_2$, or air atmospheres), the actinide cations have charges of +3 (Am, Cm) or +4 (U, Np). Plutonium occurs as $Pu^{4+}$ (air-atmosphere synthesis), $Pu^{3+}$ (synthesis under reducing conditions), or simultaneously in both forms. Similar behavior is typical of Ce (Begg *et al.*, 1998). However, Pu is more stable in tetravalent form, whereas Ce is more stable in trivalent form. Thus, we estimated the stabilities of $[^{VIII}(An^{3+})_2{}^{VI}(B^{4+})_2O_7]$ and $[^{VIII}(CaAn^{4+})^{VI}(B^{4+})_2O_7]$, where trivalent and tetravalent actinides occupy all or half of sites with CN = 8.

$[(A^{3+})_2(B^{4+})_2O_7]$ *compounds.* The ionic radii of $Pu^{3+}$, $Am^{3+}$, and $Cm^{3+}$ with CN = 8 are 1.08–1.10 Å and are close to the radii of the $Nd^{3+}$, $Pm^{3+}$, and $Sm^{3+}$ cations (Shannon, 1976). Thus, we can expect that the conditions of stability of the pyrochlore structures for compounds with the same cations in the site with CN = 6 are similar. Let us consider structural data for the $[(REE^{3+})_2(B^{4+})_2O_7]$ phases. The [6]-coordinated sites can be occupied by tetravalent cations of elements from the VI group of the periodic table with radii from 0.4 Å

($Si^{4+}$) to 0.78 Å ($Pb^{4+}$). The pyrochlore structure is not stable for all of these compounds (Toropov *et al.*, 1969; *Diagrammy sostoyaniya …*, 1985; *Rentgenovskaya baza …*, 1999). The optimal radius of an octahedrally coordinated cation is 0.65–0.69 Å. The Sn cations with radii within this interval form pyrochlore-type phases with all REEs (from La to Lu) (McCauley, 1980; *Rentgenovskaya baza …*, 1999).

A decrease (or increase) in the radius of the [6]-coordinated cation should be accompanied by corresponding changes in the radius of the [8]-coordinated cation. For example, among titanates ($[Ti^{4+}]^{IV}$ = 0.605 Å), the pyrochlore-type structure is typical of phases of medium and heavy REEs (from Sm to Lu) with relatively small ionic radii. The $Ge^{4+}$ cation has a smaller radius (0.53 Å); as a result, germanates with the pyrochlore structure include relatively small lanthanide cations (from Gd to Lu) at a pressure of 65 kbar. REE silicates with pyrochlore structure are not stable, because of the small radius of the $Si^{4+}$ cation (0.40 Å). Silicates with this structure were synthesized only for In and Sc, which have smaller ionic radii than HREEs, at a pressure of 120 kbar (McCauley, 1980).

Similarly, an increase in the radius of the cation occupying the octahedral site also affects the structure stability. For example, only compounds of the light lanthanides (from Gd to La) with the largest ionic radii among the REEs form hafnates and zirconates with pyrochlore structure (the radii of $Zr^{4+}$ and $Hf^{4+}$ are equal to 0.71–0.72 Å). Three rare-earth elements (Gd, Sm, and Nd) can form phases with pyrochlore or fluorite structures (Subramanian *et al.*, 1983). The latter structure is a more disordered high-temperature variety. The phase boundaries between the varieties of different structural types are located at 1600°C for Gd zirconate, at 2100°C for Sm zirconate, and at 2300°C for Nd zirconate. The REE plumbates have a fluorite-type structure (*Rentgenovskaya baza …*, 1999), where REE and Pb cations occupy the same sites with CN = 8. This is probably related to the large radius of the $Pb^{4+}$ cation (0.78 Å), which precludes the formation of REE plumbates with pyrochlore structure.

Thus, the radius of the B ion in the REE pyrochlores of $REE_2B_2O_7$ type can vary from 0.605 Å (Ti) to 0.72 Å (Zr). Stoichiometric compounds of this type should contain 33 mol % REEs. The real phases (particularly, higher temperature varieties) deviate from this formula. For example, the $Y_2O_3$ content in the $Y_2Ti_2O_7$ phase varies from 33 to 35 mol % at 1400°C and can increase to 32–52 mol % at 1700°C (Toropov *et al.*, 1969). $Tc^{4+}$ with a radius of 0.65 Å can also form such phases. The long-lived $^{99}Tc$ isotope is a product of $^{235}U$ fission. It is very hazardous for the environment and should also be immobilized in reliable matrices based, for example, on the pyrochlore-type structure.

The results obtained for the REE pyrochlores allow us to estimate the phase stability of trivalent actinides. On the basis of the ionic radii of actinides (Shannon, 1976), we can predict the stability of pyrochlore-type phases with Cm, Am, and Pu (Table 2). Unlike $Cm^{3+}$, the $Pu^{3+}$ and $Am^{3+}$ titanates have monoclinic symmetry as LREE titanates. This is related to their having larger ionic radii than is necessary for the pyrochlore structure. However, regardless of the instability of $Pu_2Ti_2O_7$ and $Am_2Ti_2O_7$ phases with the pyrochlore structure, pyrochlores with significant amounts of Pu and Am were synthesized (Shoup and Bambergher, 1997). They are solid solutions where lanthanide cations with smaller radii stabilize the pyrochlore structure. It was found that the pyrochlore phase based on $Gd_2Ti_2O_7$ can include 16 mol % $Pu_2Ti_2O_7$. The proportion of the $Pu_2Ti_2O_7$ end member increases with decreasing radius of the rare-earth elements up to 22 mol % in pyrochlore based on $Er_2Ti_2O_7$ and up to 33 mol % in the $Lu_2Ti_2O_7$ pyrochlore. The proportion of the Am end member in the $(Er,Am)_2Ti_2O_7$ pyrochlore solid solution is still higher (61 mol %). This result can also be obtained by replacement of Ti in octahedral sites by larger cations of Sn, Hf, and Zr, which stabilize the pyrochlore structure of the $[(Pu,Am)_2(Ti,Sn,Hf,Zr)_2O_7]$ phase.

Wastes from reprocessing of irradiated nuclear fuel are dominated by elements with more stable tetravalent cations (U, Np, Pu), only a small amount of which can be incorporated in $A_2B_2O_7$ pyrochlores (Raison *et al.*, 1999). Because of a charge difference, isomorphic substitution of actinides for REEs increases the amount of vacancies by $4REE^{3+} = 3U^{4+}$ + [vacancy], i.e., increases the deficiency of the structure. The scale of this substitution is relatively low. According to our data, the Y titanate can contain 12 wt % $UO_2$, i.e., 0.2 U atoms per formula.

The charge balance of the structure can be also maintained by substitution of two REE cations for a divalent cation (e.g., $Ca^{2+}$) and a tetravalent actinide. Such a replacement results in a pyrochlore with the formula $[^{VIII}(CaAn^{4+})^{VI}(B^{4+})_2O_7]$ with one actinide atom. Thus, the amount of actinide increases by five times compared to the previous substitution type.

$[^{VIII}(CaAn^{4+})^{VI}(B^{4+})_2O_7]$ *compounds.* Such phases can be predicted from comparison of radii of cations in REE pyrochlores $[(A^{3+})_2(B^{4+})_2O_7]$ and the effective radius of the $Ca^{2+} + An^{4+}$ pair, where An = Th, U, Np, Pu (Table 2). An effective radius of the cationic pair falling within the interval typical of a stable pyrochlore structure can indicate the possible stability of corresponding actinide compounds. The ($Ca^{2+} + U^{4+}$) and ($Ca^{2+} + Np^{4+}$) pairs, with respective effective radii of 1.06 and 1.05 Å, which are close to the radius of $Gd^{3+}$, compose many phases with $Ti^{4+}$, $Sn^{4+}$, $Zr^{4+}$, and $Hf^{4+}$ cations. Incorporation of larger (e.g., $Th^{4+}$) or smaller (e.g., $Pu^{4+}$) cations causes changes in the effective ionic radius and decreases the amount of possible pyrochlore-type compounds (Table 2). The latter are stannates, hafnates, and zirconates for Th and stannates and

**Table 2.** $[(REE)_2^{VIII}B_2^{VI}O_7]$ and $[^{VIII}(CaAn^{4+})^{VI}(B^{4+})_2O_7]$ phases of the pyrochlore type (McCauley, 1990; *Rentgenovskaya baza…*, 1999)

| $A_{VIII} = REE^{3+}$ ($r_{VIII}$, Å) | $Ti^{4+}$ ($r_{VI}$ = 0.605 Å) | $Sn^{4+}$ (0.69 Å) | $Zr^{4+}$ (0.72 Å) | $A_{VIII} = An^{3+}$ or $Ca^{2+} + An^{4+}$ ($r_{VIII}$, Å) |
|---|---|---|---|---|
| $La^{3+}$ (1.16) | | + | + | |
| $Ce^{3+}$ (1.14) | – | + | + | |
| $Pr^{3+}$ (1.13) | – | + | + | $Ca^{2+}$ (1.12) |
| $Nd^{3+}$ (1.11) | – | + | + | $Pu^{3+}$ (1.10) |
| $Pm^{3+}$ (1.09) | – | + | + | $Am^{3+}$ (1.09) |
| | – | + | + | Ca + Th (1.085) |
| $Sm^{3+}$ (1.08) | + | + | ± | $Cm^{3+}$ (1.08) |
| $Eu^{3+}$ (1.07) | + | + | ± | Ca + U (1.06) |
| $Gd^{3+}$ (1.05) | + | + | ± | Ca + Np (1.05) |
| $Tb^{3+}$ (1.04) | + | + | – | $Th^{4+}$ (1.05) |
| $Dy^{3+}$ (1.03) | + | + | – | Ca + Pu (1.04) |
| $Ho^{3+}$ (1.02) | + | + | – | |
| $Er^{3+}$ (1.00) | + | + | – | $U^{4+}$ (1.00) |
| $Tm^{3+}$ (0.99) | + | + | – | $Np^{4+}$ (0.98) |
| $Yb^{3+}$ (0.99) | + | + | – | |
| $Lu^{3+}$ (0.98) | + | + | – | $Pu^{4+}$ (0.96) |

Note: "+" denotes stability of the pyrochlore structure; "–" denotes instability of the pyrochlore structure; and "±" indicates that Sm, Eu, and Gd zirconates can have fluorite or pyrochlore-type structures.

titanates for Pu. It is theoretically possible for Ca to be replaced by Sr (1.26 Å) in $[^{VIII}(CaAn^{4+})^{VI}(B^{4+})_2O_7]$, which allows incorporation of fission products together with tetravalent actinides in a single matrix. The phase $SrPu_2Ti_4O_{12}$, with perovskite structure, was previously proposed for this purpose (Shoup and Bambergher, 1997). In fact, however, the synthesis of Sr–Th pyrochlores has not been successful (see below).

*Some other possible compounds with pyrochlore-type structure.* Based on specific features of the pyrochlore structure, $[^{VIII}(An^{4+})_2{}^{VI}(B^{3+})_2O_7]$ phases are considered to be the most stable (Chakoumakos, 1984). However, this suggestion has not yet been verified experimentally. There are many compounds with various cations in the B site that meet the requirements of charge balance and geometric stability (Aleshin and Roy, 1962; McCauley, 1980). They comprise $[(An^{3+})_2(B^{4+})_2O_7]$ and $[(CaAn^{4+})(B^{4+})_2O_7]$ with substitutions $2B^{4+} = B_1^{5+} + B_2^{3+}$, including $2Ti^{4+} = Nb^{5+}$ (or $Ta^{5+}$) + $Fe^{3+}$.

*Pyrochlore matrices with actinides.* Pyrochlore-type phases with the compositions $CaUTi_2O_7$ and $CaCeTi_2O_7$ (Ce serves as an imitator of Pu) were synthesized (Ringwood, 1985; Xu *et al.*, 2000). The phases $[Ca(Pu,U,Zr)Ti_2O_7]$ and $[Ca(Np,Zr)Ti_2O_7]$ with 45 wt % $PuO_2$ and $NpO_2$ (or 0.8–1 Pu or Np atoms per formula) were also obtained (Vance *et al.*, 1995). The titanate pyrochlore is the main phase of matrices for immobilization of wastes with high actinide content, e.g., irradiated nuclear fuel (Ringwood, 1985; Solomah *et al.*, 1986). By analogy with other materials, this ceramics was called Synroc-F (where F is an abbreviation of "fuel"). Matrices composed of 80–90% pyrochlore are considered in the United States to be the most promising forms for immobilization of excess weapons Pu (Ebbinghaus *et al.*, 1998). They are produced by cold pressing followed by sintering, under conditions similar to those of production of U–Pu mixed oxide fuel. More than 1000 samples with waste imitators (Ce, Th, U) and Pu were obtained at Lawrence Livermore National Laboratory in the United States. The optimal composition of such pyrochlore corresponds to a solid solution of $CaUTi_2O_7$, $CaPuTi_2O_7$ and $Gd_2Hf_2O_7$ in the mole proportion of 2 : 1 : 1 (Ebbinghaus *et al.*, 1998).

Melting followed by crystallization is another method of synthesizing crystalline HLW matrices. Its use was hampered for a long time because of the high liquidus temperatures of these phases, exceeding 1500°C. A technology based on inductive melting in a cold crucible was proposed to produce such matrices. This method was developed specially for synthesis of refractory materials (Aleksandrov *et al.*, 1973). Melting followed by crystallization has several advantages over the methods of solid-phase synthesis. While showing similar productivity, it is less dependent on the

**Table 3.** Phases identified in samples and their formulas

| Ideal composition | Phases identified | Pyrochlore formula |
|---|---|---|
| $CaUTi_2O_7$ | Pyr > Br | $Ca_{1.06}U_{0.72}Ti_{2.22}O_{6.94}$ |
| $CaUZr_2O_7$ | CO | Pyrochlore is not found |
| $CaCeTi_2O_7$ | Pyr > Per > CO | $Ca_{1.03}Ce_{0.99}Ti_{1.98}O_{6.98}$ |
| $CaThSn_2O_7$ | Pyr ≫ CO | $Ca_{0.92}Th_{0.92}Sn_{2.0}(Fe_{0.08})^*O_{6.96}$ |
| $SrThSn_2O_7$ | Cas > CO > Per | Pyrochlore is not found |
| $CaThZr_2O_7$ | Pyr > Per ~ CO | $Ca_{0.91}Th_{0.84}Zr_{2.25}O_{7.09}$ |
| $SrThZr_2O_7$ | Per > CO | Pyrochlore is not found |
| $(Ca_{0.5}GdTh_{0.5})Zr_2O_7$ | Pyr ≫ CO | $(Ca_{0.44}GdTh_{0.42})Zr_{2.13}O_{7.05}$ |
| $(Ca_{0.5}GdU_{0.5})Zr_2O_7$ | CO | Pyrochlore is not found |
| $(Ca_{0.5}GdU_{0.5})(ZrTi)O_7$ | Pyr > CO | $(Ca_{0.62}Gd_{0.97}U_{0.23})(Zr_{0.84}Ti_{1.34})O_{6.90}$ |
| $(Ca_{0.5}GdTh_{0.5})(ZrTi)O_7$ | Pyr ≫ CO | $(Ca_{0.47}Gd_{0.95}Th_{0.4})(Zr_{1.29}Ti_{0.89})O_{7.05}$ |

Note: Pyr, phase with pyrochlore structure; Br, uranium titanate (brannerite); CO, oxide with fluorite structure; Per, phase with perovskite structure; Cas, Sn oxide (cassiterite).

* Contamination from grinding of starting material.

reduction and homogeneity of the starting material. Relics of unreacted starting material, which are usual in products, of solid-phase synthesis are unlikely in products of melting and crystallization. Pyrochlore $CaUTi_2O_7$ was synthesized using this technique (Stefanovsky *et al.*, 1999). The nonstoichiometry found in its composition is expressed in the excess of Ca over U as compared to the theoretical formula.

We can suggest that the probable pyrochlore matrices for HLWs should incorporate actinides, Zr, REE, and neutron absorbers (Gd, Sm, and Hf). Their compositions correspond to $x[(CaAn^{4+})B_2O_7] + (1 - x)[(REEAn^{3+})_2B_2O_7]$, where B are cations from Ti to Zr and the coefficient $x$ depends on the amount of tetravalent actinides in the HLW. We attempted to synthesize new pyrochlore-type actinide phases based on titanates, stannates, and zirconates. The latter are most interesting because of their higher resistance to radiation as compared with titanates (Wang *et al.*, 1999).

## SYNTHESIS AND STUDY OF NEW PYROCHLORE MATRICES FOR ACTINIDES

Starting material with the composition $[(A_1^{2+}A_2^{4+})_2(B^{4+})_2O_7]$, where $A_1^{2+}$ = Ca or Sr; $A_2^{4+}$ = U or Th; and $B^{4+}$ = Ti, Sn, or Zr, was prepared of element oxides disintegrated to 20–30 μm. The powders were pressed at 200–400 MPa into cylindrical pellets 4–5 mm high and 12–20 mm in diameter. These pellets were placed into alundum crucibles and sintered at 1500–1550°C for 2–20 h. The grinding and sintering were repeated in some cases. Sample equilibration was recognized according to invariable phase composition of final product with an increase the sintering time. The samples were studied using X-ray powder diffraction (DRON-3, Cu irradiation) and scanning (JSM-5300 and JSM-6510LV) and transmission (JEM-100C) electron microscopy.

The pyrochlores with Ti and Sn form most rapidly, while the slowest synthesis is characteristic of zirconate systems (Laverov *et al.*, 2002). Pyrochlore is the major or single phase in most of the samples studied (Table 3). The titanate matrices also contain brannerite, perovskite, and a fluorite-type oxide. Pyrochlore in the zirconate matrices is found only in the Th-bearing samples. The replacement of Th by U in zirconates is accompanied by the formation of a fluorite-type oxide instead of pyrochlore (Table 3, Fig. 1).

Pyrochlores were synthesized for the first time, except for the phases in the Ca–U–Ti–O and Ca–Ce–Ti–O systems. Data on these phases is absent in the X-ray diffraction databases. Their common feature is a deficiency of cations in the [8]-coordinated site of their formulas (Table 3). A part of $Zr^{4+}$ cations could also occupy the [8]-coordinated sites. The divalent Ca cations, rather than the tetravalent actinides are preferably located in the [8]-coordinated sites. The substitution of U for Th in $CaThZr_2O_7$ and $(Ca_{0.5}GdTh_{0.5})Zr_2O_7$ matrices makes the pyrochlore structure unstable (Table 3, Fig. 1). This is probably related to smaller radius of $U^{4+}$ (1.0 Å) as compared to radius of $Th^{4+}$ (1.05 Å). As a result, the ratio of ionic radii in the $^{VIII}[A]$ and $^{VI}[B]$ sites decreases beyond the range characteristic of pyrochlore-type structures. The replacement of Zr cations by smaller Ti cations increases this ratio and stabilizes the pyrochlore structure for the $[(CaU)(ZrTi)O_7]$ and $[(Ca_{0.5}GdU_{0.5})(ZrTi)O_7]$ compounds. Sr–Th pyrochlores have not been synthesized, even with large $Sn^{4+}$ and $Zr^{4+}$ cations in the [6]-coordinated site (Table 3), regardless of the formal consistence of the ratio of ionic radii to the requirements of geometrical stability. Oxides with fluorite and perovskite structures, as well as Sn oxide, were obtained instead of pyrochlore from

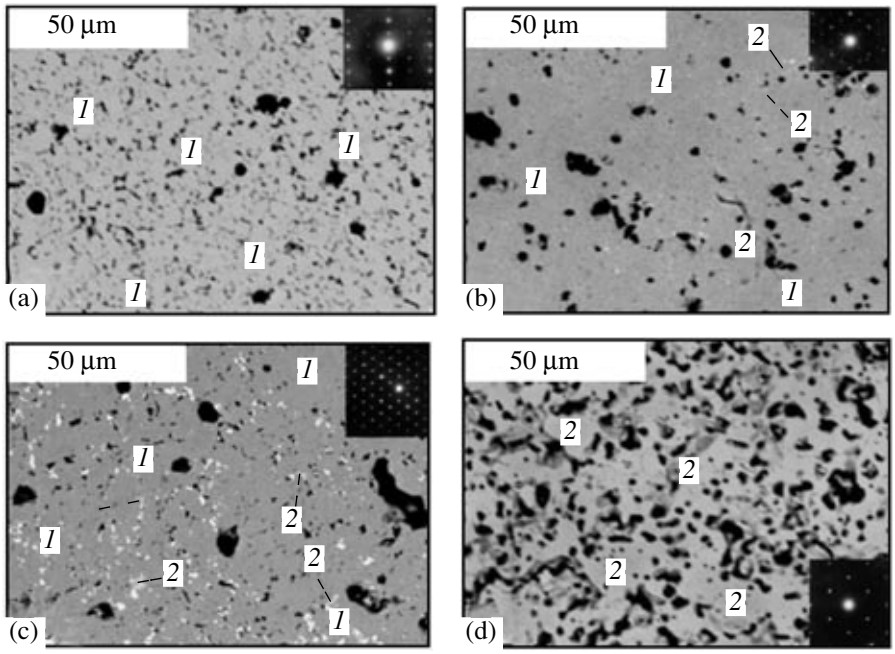


**Fig. 1.** BSE images of samples of the following compositions: $CaThSn_2O_7$ (a), $(Ca_{0.5}GdTh_{0.5})Zr_2O_7$ (b), $(Ca_{0.5}GdTh_{0.5})(ZrTi)O_7$ (c), and $CaUZr_2O_7$ (d). (*1*) Phase with pyrochlore structure; (*2*) oxide with fluorite structure; black spots are pores. Insets show images of electron microdiffraction from planes of reciprocal lattices of pyrochlore (upper right corner) and fluorite types (lower right corner).

starting materials with stoichiometries of $SrThSn_2O_7$ and $SrThZr_2O_7$.

Data on correlation of composition with structure should be taken into account in selecting matrices for actinide-bearing wastes, particularly for compositionally complex wastes, e.g., the actinide–Zr–REE fraction of HLWs. The octahedrally coordinated cations of pyrochlore phases with REE and trivalent actinides vary in radii from 0.55 to 0.75 Å. The $Ti^{4+}$, $Sn^{4+}$, $Hf^{4+}$ and $Zr^{4+}$ ionic radii are within this interval. $Tc^{4+}$, with an ionic radius of 0.65 Å, can also occupy the octahedral sites. Its long-lived isotope $^{99}Tc$, forming during $^{235}U$ fission with a yield of 6% (Roedder, 1990), can also be incorporated into the pyrochlore matrix. The capacity of the pyrochlore structure to incorporate tetravalent actinides increases if it simultaneously includes $Ca^{2+}$ cations as compensators of excess charge.

However, pyrochlore-type phases, capable of incorporating large amount of actinides, show limited capacity to include the other components of HLWs. This can result in the formation of additional phases, reducing the insulative properties of the matrix. Thus, the selection of crystalline phases for immobilization of complex wastes from reprocessing of irradiated nuclear fuel is an important task. These wastes contain significant amounts of Fe, Al, Ga, Si, and some other elements (Burakov *et al.*, 1999). Compounds with a garnet structure are promising materials for their immobilization.

## GENERAL INFORMATION ON GARNET STRUCTURE

The garnet structure was interpreted by Menzer (1928) for grossular, a natural mineral with the formula $Ca_3Al_2Si_3O_{12}$. This structure was then repeatedly refined for natural minerals and synthetic compounds (Geller, 1967). This structure is typical of phases with the formula $A_3^{VIII}B_2^{VI}X_3O_{12}$ (*Ia3d*, $Z = 8$) and is a framework of alternating $XO_4$ tetrahedra and $BO_6$ octahedra sharing common vertices. The interstices, distorted cubes (triangle dodecahedra) in shape, are occupied by large cations. The existence of three sites, A, B, and X, with CN = 8, 6, and 4, respectively, allows potential incorporation of various elements in the garnet structure. The $[A]^{VIII}$ site normally includes divalent (Ca, Mn, Mg, Fe, Co, Cd) and trivalent (Y, REE) cations. Trivalent (Fe, Al, Ga, Cr, Mn, In, Sc, N) and tetravalent (Zr, Ti, Sn) cations occupy the $[B]^{VI}$ site. The $[X]^{VI}$ site is filled with trivalent (Al, Ga, Fe), tetravalent (Ge, Si), and pentavalent (V, As) cations.

*Natural garnets.* The natural garnets are generally silicates. Their compositions vary widely due to different isomorphic substitutions. The garnet compositions are described as mixtures of simple compounds or end members (Deer et al., 1965; Rickwood, 1968). The following two garnet series are distinguished: ugrandites ($[A]^{VIII} = Ca^{2+}$) and pyralspites ($[B]^{VI} = Al^{3+}$). The ugrandites include calcic garnet as mixtures of uvarovite, grossular, and andradite. The pyralspites are aluminous garnets as mixtures of pyrope, almandine, and spessar-

**Table 4.** Stability of garnets $[(REE^{VIII})_3(B^{VI})_2(X^{IV})_3O_{12}]$, where B = X = $Al^{3+}$, $Ga^{3+}$, or $Fe^{3+}$ (Toropov *et al*., 1969)

| Lanthanides ($r_{VIII}$, Å) | $Al^{3+}$ ($r_{IV}$ = 0.39 Å, $r_{VI}$ = 0.545 Å) | $Ga^{3+}$ ($r_{IV}$ = 0.47 Å, $r_{VI}$ = 0.62 Å) | $Fe^{3+}$ ($r_{IV}$ = 0.49 Å, $r_{VI}$ = 0.65 Å) | Actinides ($r_{VIII}$, Å) |
|---|---|---|---|---|
| La (1.16) | – | – | ? | |
| Pr (1.13) | – | ? | ? | |
| Nd (1.11) | – | + | ? | $Am^{3+}$ (1.09) |
| Sm (1.08) | – | + | + | $Cm^{3+}$ (1.08) |
| Eu (1.07) | – | + | + (1460**°C) | |
| Gd (1.05) | – | + (1740*°C) | + (1460**°C) | |
| Dy (1.03) | + (1920*°C) | + | + | |
| Y (1.02) | + (1940*–1760**°C) | + | + (1570*–1470**°C) | |
| Ho (1.02) | + (1950*°C) | + | + | |
| Er (1.00) | + (1960*°C) | + | + | |
| Yb (0.99) | + (2000*°C) | + | + | |
| Lu (0.98) | + (2060*°C) | + | + | |

Note: "+" denotes stability of the garnet structure; "–" denotes instability of the garnet structure; "?" indicates that no data were available.
* Melting temperature of garnet.
** Eutectic temperature mixture of garnet with oxide ($Al_2O_3$, $Ga_2O_3$, or $Fe_3O_4$).

tine. They contain $Al^{3+}$ cations in the [B] site and divalent Mg, Mn, and Ca in the [A] site. The end members form continuous solid solutions within each series, whereas miscibility between end members of different series is limited. Rare natural garnets have high Zr (kimzeyite), Ti (schorlomite), and V (goldmanite) contents. Kimzeyite contains up to 30 wt % $ZrO_2$ (Dowty, 1971; Schingaro *et al.*, 2001) and the Si content can decrease below one atom per formula unit. Nonsilicate natural garnets are also known, i.e., berzeliite $(NaCa_2)Mn_2As_3O_{12}$ and cryolithionite $Na_3Al_2Li_3F_{12}$.

*Relation of structural and chemical features of garnet-type phases.* The garnet structure is stable in the case of a certain relation between charges and radii of ions in different sites (Geller, 1967; Mill' and Roniger, 1973, etc.). The cation–anion relation must meet the charge balance requirement. A certain relation between ionic radii is another factor in structure stability. The geometrical principles of stability of the garnet structure are based on analysis of silicate garnet structures (Novak and Gibbs, 1971). More than 200 combinations of cationic pairs were considered, and the field of silicate garnet stability was determined in the coordinates of radii of cations in the A and B sites. The radii of cations in these two sites should concurrently increase. A disturbance of these requirements leads to the formation of a compound with a different structure. However, not all garnets that could be stable according to geometrical analysis can be synthesized at atmospheric pressure. Many of them can only be obtained at elevated pressures, which should be higher the difference the higher between the radii of the [8]- and [6]-coordinated cations (Nishizawa and Koizumi, 1975; Fursenko, 1980, 1983).

A change in size of the cation in the X site also transforms the stability of the garnet structure (Geller, 1967). With an increase (or decrease) in the size of this cation, the radii of the cations in the A and B sites should also correspondingly increase (or decrease). For example, germanates are stable in the presence of larger [6]- and [8]-coordinated cations as compared to silicates (Mill' *et al.*, 1982). Similarly, an increase in the radius of the cation in the X site in the sequence of $Al^{3+}$–$Ga^{3+}$–$Fe^{3+}$ makes the garnet structures with larger cations in the A and B sites more stable (Table 4). These tendencies have been verified experimentally.

The garnet structure can be stabilized by addition of elements that change the effective radius of cations in a site. For example, grossular ($Ca_3Al_2Si_3O_{12}$) cannot be synthesized at atmospheric pressure. However, a garnet with composition $[Ca_3(Al_{1.33}Cr_{0.67})Si_3O_{12}]$, where one-third of the Al atoms are replaced by Cr, has been synthesized (Gentile and Roy, 1960). A similar effect is observed on addition of Y and Fe oxides (Geller and Miller, 1959). A continuous solid solution from 90 mol % $Ca_3Al_2(SiO_4)_3$ + 10 mol % $Y_3Fe_2(FeO_4)_3$ to 100 mol % $Y_3Fe_2(FeO_4)_3$ with garnet structure occurs at 1 atm and 1400°C. The replacement of Y by Gd reduces solubility of the grossular end member in the garnet to 10 mol %. This is probably related to the larger radius of the $Gd^{3+}$ cation (1.05 Å) as compared to the $Y^{3+}$ cation (1.02 Å), which makes $Gd^{3+}$ a less efficient stabilizer of the garnet structure.

*Possible actinide phases of the garnet type.* Natural garnets contain up to a few fractions of percent of U and Th and up to a few percent of REE (Jaffe, 1951; Schingaro *et al.*, 2001). Thus, unlike the pyrochlore-type phases hosting actinides, the study of natural garnets

does not allow estimation of actinide and lanthanide solubility in the garnet structure and selection of compositions that could serve as HLW matrices. To obtain such information, let us consider the available experimental data.

Because of their sizes, the trivalent and tetravalent actinide and REE cations generally occupy large dodecahedral interstices in the structure. The combination of polyhedra in the crystal structure determines the relation between sizes of cations in the different structural sites. The effect of the structural factor on the chemical composition of REE garnets is obvious (Toropov *et al.*, 1969). There are aluminate, gallate, and ferrite phases ($REE_3B_2X_3O_{12}$) among them, where B = X = $Al^{3+}$, $Ga^{3+}$, or $Fe^{3+}$ (Table 4). The radii of cations in the [4]- and [6]-coordinated sites increase in the following sequence: 0.39 Å (IV) and 0.54 Å (VI) for $Al^{3+}$, 0.47 Å (IV) and 0.62 Å (VI) for $Ga^{3+}$, and 0.49 Å (IV) and 0.65 Å (VI) for $Fe^{3+}$. For the stability of the structure, the increase in the cation radii in the $[B]^{VI}$ and $[X]^{IV}$ sites should be accompanied by an increase in the cation radius in the $[A]^{VIII}$ site. According to this rule, the sizes of cations in the dodecahedral site should increase in the above compositional series. It was found (Table 4) that the aluminate garnets are stable with REEs from $Lu^{3+}$ to $Dy^{3+}$ with radii from 0.98 to 1.03 Å. The garnet structure for gallates is stable up to $Nd^{3+}$ (1.09 Å). If the cation radius is beyond this range, a phase with perovskite structure and an oxide form instead of garnet: $REE_3B_5O_{12} = 3\ REEBO_3 + B_2O_3$, where B = $Al^{3+}$, $Ga^{3+}$, $Fe^{3+}$ (Toropov *et al.*, 1969). The melting temperature of ferrites is about 400°C lower than that for aluminates and 200°C lower than that for gallates (Table 4). The temperature of ferrite garnet and oxide eutectic with 35 mol % (~70 wt %) garnet is still lower (~1460°C). Lower melting temperatures facilitate the synthesis of HLW matrices by the melting and crystallization technique.

Based on the similarity in cationic sizes of $Am^{3+}$ with $Cm^{3+}$ and $Gd^{3+}$ with $Nd^{3+}$, we could expect similar behavior of these elements in synthesis of garnet matrices. The garnet structure is most probable for ferrites and gallates of trivalent actinides. Incorporation of tetravalent actinides in garnet was experimentally tested for Th (Ito and Frondel, 1967). They synthesized garnet from mixtures $(Ca_{2.5}Th_{0.5})Zr_2Fe_3O_{12}$ and $(Ca_2Th)(ZrFe)Fe_3O_{12}$ at $T$ = 1050 and 1200°C and 1 atm pressure. The products were studied only by X-ray powder diffraction. A monophase garnet ceramics was formed from the starting material $[(Ca_{2.5}Th_{0.5})Zr_2Fe_3O_{12}]$. A monophase garnet ceramics was also obtained from the composition $[(Ca_2Th)(ZrFe)Fe_3O_{12}]$ at 1050°C, whereas garnet associates with Th dioxide at 1200°C. Garnet with Th replaced by Ce, i.e., $[(Ca_{2.5}Ce^{4+}_{0,5})Zr_2Fe_3O_{12}]$, was also synthesized.

The published data on the composition of Th and Ce garnets were obtained by an indirect method, i.e., from the suggestion that the synthesized garnet corresponds to the starting material by stoichiometry (i.e., the proportions of components in the starting material characterize the composition of the final product), because garnet was found to be a single phase in the synthetic product. However, this suggestion should be examined using methods of local analysis. The above study did not consider the properties of the synthesized garnet as matrix material for immobilization of actinide-bearing wastes. Special-purpose studies initiated within the last 10–15 years are aimed at the solution of this problem.

## EXPERIMENTAL STUDY OF GARNET MATRICES FOR HIGH-LEVEL RADIOACTIVE WASTES

Specialists from the Research Institute of Inorganic Materials were the first to propose garnet for HLW immobilization (Vlasov *et al.*, 1987; Nikiforov *et al.*, 1992). They synthesized materials close in composition to andradite ($Ca_3FeSi_3O_{12}$) by inductive melting in a cold crucible. However, the phase and chemical compositions of these materials have not been determined, and, therefore, the formation of garnet has not been proved. These studies were continued later and resulted in the synthesis of a matrix containing more than 80% garnet (Smelova *et al.*, 2000). The concentration of REE and Zr oxides reached 20 wt %. However, actinide incorporation in the matrix has not been defined.

The study of garnet ceramics as potential matrices for actinide immobilization is being carried out by specialists of the Radium Institute (Burakov *et al.*, 1999, 2000; Burakov and Anderson, 2002). The basic phase for the study is a REE (Y, Gd) aluminate–gallate garnet. Ce and U oxides or more complex mixtures modeling wastes of Pu production serve as HLW imitators. Polyphase ceramics of the garnet-, perovskite- and hibonite-type phases, as well as rare Zr and Al oxides, are products of the experiments. The chemical compositions of the samples affect their phase composition. Perovskite dominates in the $Gd_2O_3$–$Al_2O_3$ system. Garnet is the major phase in the $Gd_2O_3$–$Ga_2O_3$ system and contains about 6 wt % Ce and <0.1 wt % U. Addition of metallic Sn (4 wt %) in the starting material increases the U content in garnet up to 5.5 wt %. Garnet includes <10% of the total uranium amount of the sample. Plutonium shows similar solubility in garnet (about 6 wt %) (Burakov *et al.*, 2000). Thus, REE–Al–Ga garnets have a low capacity to incorporate U, Pu, and Ce and cannot be recommended for immobilization of HLWs with high actinide contents. However, these results do not preclude the use of garnet ceramics as matrices for actinide immobilization. They only indicate that comprehensive studies of garnet structure are necessary to find appropriate materials.

It was demonstrated (Yudintsev *et al.*, 2002) that ferrite garnets could have the highest capacity to incorporate tetravalent actinides. The radii of the $Th^{4+}$ and

**Table 5.** Calculated garnet formulas and compositions of experimental products

| Sample | Theoretical (calculated) formula | Phases in ceramics |
|---|---|---|
| 3-U | $(Ca_{1.5}GdU_{0.5})(ZrFe)Fe_3O_{12}$ | Gar > CO > Hib |
| 3-Th | $(Ca_{1.5}GdTh_{0.5})(ZrFe)Fe_3O_{12}$ | Gar |
| 45-Ce | $(Ca_{1.5}GdCe_{0.5})(ZrFe)Fe_3O_{12}$ | Gar ≫ Per |
| 1-Pu | $(Ca_{1.5}GdPu_{0.5})(FeZr)Fe_3O_{12}$ | Gar ≫ Hib |
| 4-Th | $(Ca_{2.5}Th_{0.5})Zr_2Fe_3O_{12}$ | Gar ≫ Per > CO |
| 21-Ce | $(Ca_{2.5}Ce_{0.5})Zr_2Fe_3O_{12}$ | Gar ≫ Per |
| 3-Th-a | $(CaGdTh_{0.5}Zr_{0.5})Fe_2(Fe_{0.5}Al_{2.5})O_{12}$ | Gar > Hib ~ CO |
| 13-Th | $(CaGd_2)(Th_{0.25}Zr_{0.25}Fe_{1.5})(Fe_{2.5}Si_{0.5})O_{12}$ | $Gar^1 > Gar^2$ |

Note: Gar, garnet; CO, cubic oxide with fluorite structure; Hib, hibonite $[Ca(Fe,Al)_{12}O_{19}]$; Per, perovskite ($CaZrO_3$).

$Ce^{4+}$ cations are 1.05 and 0.97 Å, respectively. The $Pu^{4+}$ radius (0.96 Å) is close to the $Ce^{4+}$ radius, and the ionic radii of $Np^{4+}$ (0.98 Å) and $U^{4+}$ (1.0 Å) are between those for $Th^{4+}$ and $Ce^{4+}$. This suggests that $[(Ca_{2.5}An^{4+}_{0.5})Zr_2Fe_3O_{12}]$ garnets, where An = Pu, Np, or U, can also be obtained in experiments. In order to test this suggestion, we produced ceramics in the $CaO–Al_2O_3–SiO_2–Fe_2O_3–ZrO_2–Gd_2O_3–CeO_2–UO_2–ThO_2–PuO_2$ system. The starting materials, corresponding in composition to ideal garnet stoichiometry (Table 4), were pressed at 200–400 MPa into pellets 2–3 mm high and 10 mm in diameter. Synthesis was carried out in an alundum crucible in air (or in oxygen atmosphere for Ce compositions) following the procedure of heating to 1300–1500°C with a rate of 10 K/min, holding at this temperature for 1–20 h, and cooling to room temperature. The time for attaining equilibrium was 5 h at 1300°C, 2 h at 1400°C, and 1 h at 1500°C. Some samples heated at 1500°C were melted, with the formation of a layer 3–5 mm thick at the crucible bottom. Other samples preserved the pelletal shape, which indicates higher melting temperatures.

All samples studied contain from 70–100% garnet (Table 5). Two garnets with different compositions were synthesized in one experiment (no. 13-Th) (Table 5). The strongest lines in the X-ray diffraction diagrams are located within the following ranges: 3.05–3.15 Å ($d_{400}$), 2.72–2.82 Å ($d_{420}$), 2.49–2.57 Å ($d_{422}$), which indicates significant variation of the unit cell parame-

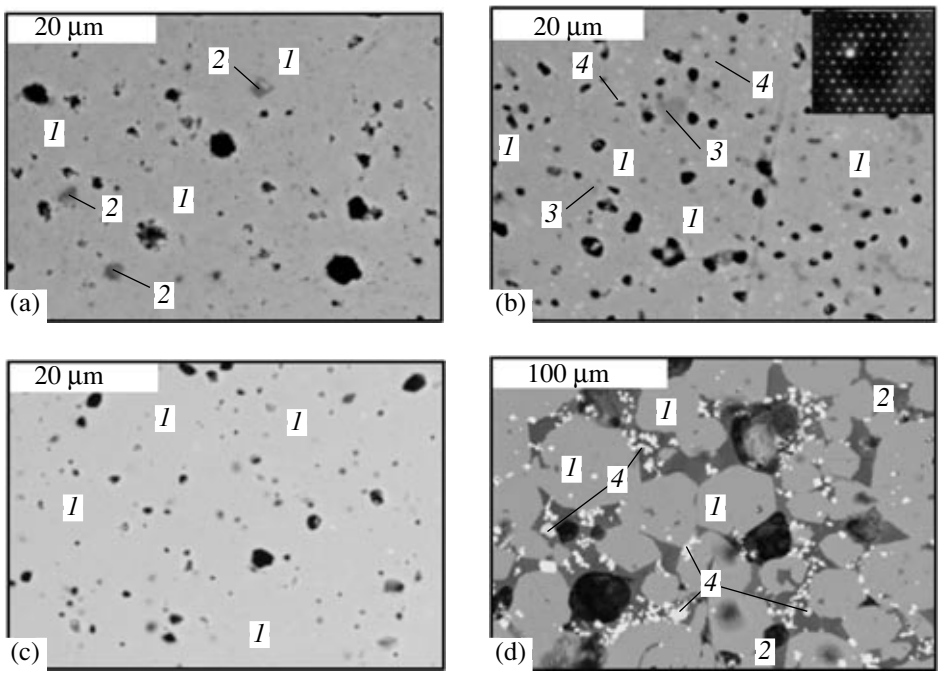


**Fig. 2.** BSE images of the following samples: 45-Ce (a), 4-Th (b), 21-Ce (c), and 3-Th-a (d). (*1*) Phase with garnet structure; (*2*) hibonite; (*3*) perovskite-type phase; (*4*) oxide with fluorite structure; black spots are pores. Insets show images of electron microdiffraction from planes of reciprocal lattices of garnet.

**Table 6.** Compositions (wt %) and probable garnet formulas in samples

| Sample | CaO | $Al_2O_3$ | $SiO_2$ | $Fe_2O_3$ | $ZrO_2$ | $Gd_2O_3$ | $UO_2$ | $ThO_2$ | $CeO_2$ |
|---|---|---|---|---|---|---|---|---|---|
| 3-U | 10.5 | 7.3 | – | 24.2 | 22.8 | 32.6 | 2.6 | – | – |
| | $(Ca_{1.48}Gd_{1.42}U_{0.08})^{VIII}(Zr_{1.47}Fe_{0.53})^{VI}(Fe_{1.87}Al_{1.13})^{IV}O_{12}$ | | | | | | | | |
| 3-Th | 10.5 | – | – | 37.3 | 16.1 | 21.2 | – | 14.9 | – |
| | $(Ca_{1.56}Gd_{0.98}Th_{0.47})^{VIII}(Zr_{1.09}Fe_{0.91})^{VI}(Fe_{2.99})^{IV}O_{12}$ | | | | | | | | |
| 45-Ce | 11.1 | – | – | 38.1 | 17.6 | 24.0 | – | – | 9.2 |
| | $(Ca_{1.58}Gd_{1.06}Ce_{0.36})^{VIII}(Ce_{0.07}Zr_{1.14}Fe_{0.79})^{VI}(Fe_{3.01})^{IV}O_{12}$ | | | | | | | | |
| 4-Th | 19.0 | – | – | 31.0 | 32.8 | – | – | 17.2 | – |
| | $(Ca_{2.57}Th_{0.49})^{VIII}(Zr_{2.02})^{VI}(Fe_{2.94})^{IV}O_{12}$ | | | | | | | | |
| 21-Ce | 19.9 | – | – | 33.7 | 33.9 | – | – | – | 12.5 |
| | $(Ca_{2.53}Ce_{0.47})^{VIII}(Ce_{0.05}Zr_{1.96})^{VI}(Fe_{3.01})^{IV}O_{12}$ | | | | | | | | |
| 3-Th-a | 10.3 | 11.1 | – | 21.7 | 18.5 | 31.2 | – | 7.2 | – |
| | $(Ca_{1.44}Gd_{1.35}Th_{0.21})^{VIII}(Zr_{1.18}Fe_{0.82})^{VI}(Fe_{1.31}Al_{1.71})^{IV}O_{12}$ | | | | | | | | |
| 13-Th | 4.3 | – | 0.6 | 30.9 | 2.9 | 45.3 | – | 16.0 | – |
| | $Gar^1 : (Ca_{0.75}Gd_{2.25})^{VIII}(Gd_{0.21}Th_{0.60}Zr_{0.23}Fe_{0.96})^{VI}(Fe_{2.85}Si_{0.10})^{IV}O_{12}$ | | | | | | | | |
| | 7.6 | – | 4.2 | 37.4 | 7.7 | 39.9 | – | 3.2 | – |
| | $Gar^2 : (Ca_{1.11}Gd_{1.81}Th_{0.10})^{VIII}(Zr_{0.52}Fe_{1.48})^{VI}(Fe_{2.38}Si_{0.58})^{IV}O_{12}$ | | | | | | | | |

Note: The occurrence of aluminum is related to dissolution of the alundum crucible in the melt. The formulas are calculated with the suggestion that all Fe occurs in a trivalent form, and U and Ce in a tetravalent form.

ters. The samples also contain actinide oxides of fluorite-type and Ca–Zr oxide with a perovskite structure, as well as Ca, Fe, and Al oxide (hibonite). Sintered and melted ceramics of similar chemical compositions are generally comparable in textural features. The samples obtained by melting and crystallization have some coarser (10–100 μm against 1–20 μm) and more euhedral grains (Fig. 2). Products of shorter (1–2 h) and relatively low-temperature (1300°C) experiments preserve up to 10 vol % oxides, indicating that the synthesis reactions have not been completed. Components of the starting materials have not been found in samples sintered for 5 h and longer.

Analytical data (Table 6) show the significant capacity of the ferrite garnets to incorporate REE (Gd, Ce), Zr, and actinides. The actinide contents are the highest (16–18 wt %) in Ca–Zr–Fe garnet and decrease with addition of Al and, particularly, Si. The decrease in

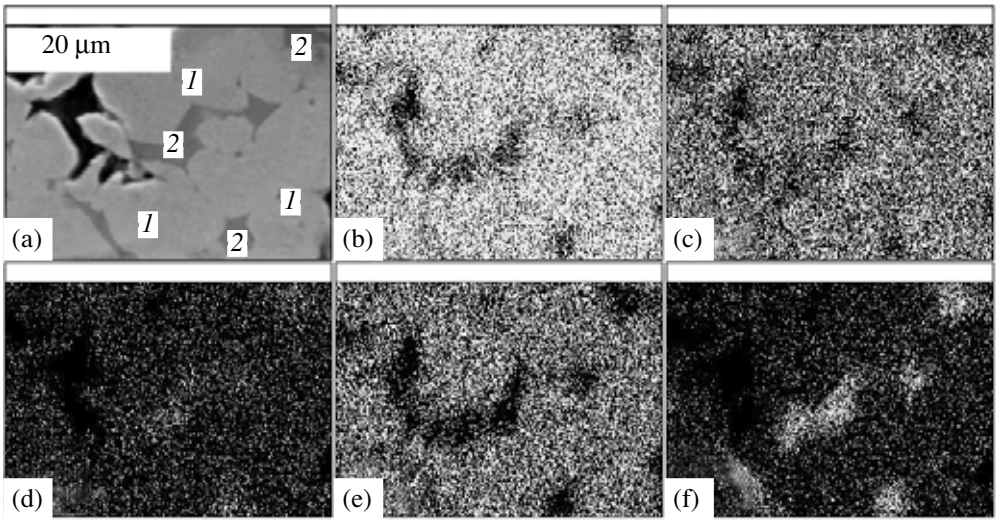


**Fig. 3.** BSE images of a sample of 1-Pu (a) and distribution of elements in this sample in the characteristic X-ray emission images of (b) Zr$L_\alpha$, (c) Pu$M_\alpha$, (d) Ca$K_\alpha$, (e) Gd$L_\alpha$ and (f) Fe$K_\alpha$. (*1*) Garnet; (*2*) hibonite; black spots are pores.

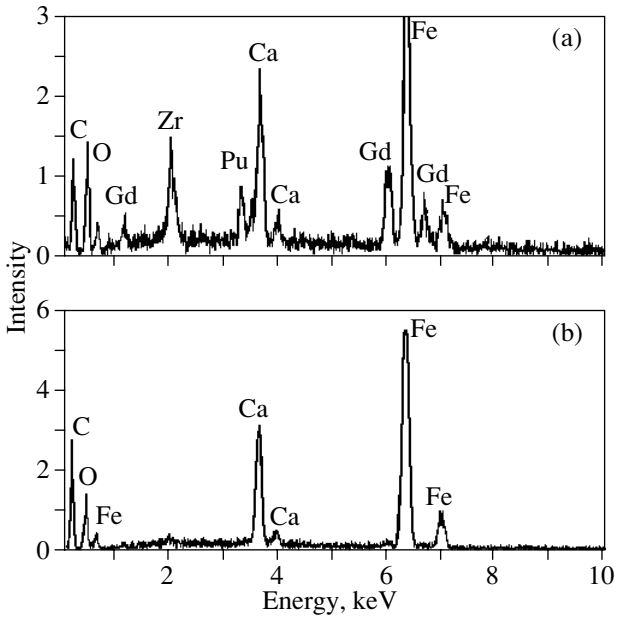


**Fig. 4.** Energy-dispersive spectra of garnet (a) and hibonite (b) in a sample of 1-Pu. The carbon peak (C) is related to the graphite film of the sample surface.

actinide concentrations is probably related to the decrease in sizes of all structural sites with replacement of $Fe^{3+}$ in the tetrahedron by the smaller $Al^{3+}$ and $Si^{4+}$ cations. Contraction of structural polyhedra hampers incorporation of large actinide cations. This is clearly expressed in the formation of two coexisting garnet phases with different actinide contents in experiment no. 13-Th. The Th concentration is five times lower in the phase with a higher Si content. The excess amount of Th is bound in thorianite (Fig. 2). Only garnet and hibonite are found in the Pu-bearing sample. The entire amount of Pu in this sample (16 wt %) is incorporated in the garnet phase (Figs. 3, 4).

## CONCLUSION

On the example of pyrochlore- and garnet-type phases, we considered employment of structural analysis in selection of optimal matrices for immobilization of actinide-containing HLWs of various compositions. The existence of several sites (two for pyrochlore and three for garnet) that could be occupied by cations with various charges and radii offers possibilities for incorporation of radioactive waste components, including actinides. Conditions of stability of the pyrochlore structure are considered for the phases $A_2B_2O_7$ and $(CaA)B_2O_7$, where A are lanthanides or trivalent and tetravalent actinides and B are tetravalent cations of elements of group IV of the periodic table. Among titanates, the pyrochlore structure is typical of medium and heavy lanthanides (from Sm to Lu) with small ionic radii. Among hafnates and zirconates, the pyrochlore structure is characteristic of the larger lanthanide atoms (from La to Gd). Data on the stability of REE pyrochlores allow us to estimate the stability of similar actinide phases. The radii of $Pu^{3+}$, $Am^{3+}$ and $Cm^{3+}$ are close to those of $Nd^{3+}$, $Pm^{3+}$, and $Sm^{3+}$. Thus, the actinide compounds with the same (as for the REE phases) cation in the octahedral site can have a pyrochlore structure. $Tc^{4+}$, with the ionic radius of 0.65 Å, can also occupy the octahedral sites. Its isotope $^{99}Tc$, forming during $^{235}U$ fission, can also be incorporated into the pyrochlore phase.

Only a small amount of tetravalent actinides can be incorporated in $A_2B_2O_7$ pyrochlores. Charge compensators (e.g., $Ca^{2+}$ ions) should be introduced to increase actinide solubility. In the resulting compounds, trivalent cations are replaced by a pair consisting of one divalent and one tetravalent cation according to the following scheme: $2REE^{3+} = Ca^{2+} + Ce^{4+}$ ($U^{4+}$, $Th^{4+}$, $Np^{4+}$, $Pu^{4+}$). Comparison of the radii of these pairs and $REE^{3+}$ cations suggests the existence of several phases of tetravalent actinides with pyrochlore structure. The average radii of the pairs ($Ca^{2+} + U^{4+}$) and ($Ca^{2+} + Np^{4+}$) are close to the radius of $Gd^{3+}$. $Pm^{3+}$ or $Sm^{3+}$ are analogues for the pair $Ca^{2+}$ and $Th^{4+}$, and $Tb^{3+}$ for the pair containing $Ce^{4+}$ or $Pu^{4+}$.

Successful synthesis of several actinide phases with the pyrochlore structure, such as $CaThSn_2O_7$, $CaThZr_2O_7$, $[(Ca_{0.5}GdTh_{0.5})Zr_2O_7]$, $[(Ca_{0.5}GdU_{0.5})(ZrTi)O_7]$, and $[(Ca_{0.5}GdTh_{0.5})(ZrTi)O_7]$, verified this suggestion. However, the $CaUZr_2O_7$, $SrThSn_2O_7$, $SrThZr_2O_7$, and $[(Ca_{0.5}GdU_{0.5})Zr_2O_7]$ phases have not been synthesized, probably because of unconformity of the ionic radii to the conditions of stability of the pyrochlore structure. Phases with fluorite- and perovskite-type structures, as well as $SnO_2$, form instead of the pyrochlore-type phases.

This paper also consideres the conditions of formation of HLW matrices with garnet-type structures. Incorporation of actinide cations ($U^{4+}$, $Th^{4+}$, $Np^{4+}$, $Pu^{4+}$) in garnet is facilitated by the existence of large cations with low valence, e.g., $Fe^{3+}$ ($r_{IV} = 0.49$ Å, $r_{VI} = 0.65$ Å), in the $[X]^{IV}$ and $[B]^{VI}$ sites. It was found experimentally that the content of actinides in garnet varies from 0.6–0.8 to 16–18 wt % and depends on the garnet composition. The highest concentrations are typical of ferrite garnets, while the lowest contents are observed for silicate and aluminate garnets.

The data obtained suggest that the pyrochlore matrices can be used for immobilization of elements of the actinide and actinide–Zr–REE fractions of HLWs. Phases with garnet structure can be used for immobilization of actinide wastes of complex composition with high contents of corrosion products (Al, Ga, Fe). We plan to study the stability of these phases to radiation and chemical corrosion.

## ACKNOWLEDGMENTS

The author thanks A.G. Ptashkin (Radon Scientific Industrial Association, Moscow) for assistance in the synthesis of matrices and L.A. Kochetkova, M.I. Lapina, A.V. Mokhov, and A.V. Sivtsov (Institute of Geology of Ore Deposits, Petrography, Mineralogy, and Geochemistry, Russian Academy of Sciences, Moscow) for their work with X-ray powder diffraction and scanning and transmission microscopy studies.

The study was supported by the Russian Foundation for Basic Research, project no. 02-05-64008, and the United States Department of Energy, project no. RC0-20002-SC14.

## REFERENCES

Actinide and Fission Product Partitioning and Transmutation, *Proc. V Int. Information Exchange Meeting*, Paris: *Nuclear Energy Agency,* 1999, EUR 18898 EN.

Aleksandrov, V.I., Osiko, V.V., Prokhorov, A.M., and Tatarintsev, V.M., New Method for Obtaining High-Melting Monocrystals and Melted Ceramic Materials, *Vestn. Akad. Nauk SSSR*, 1973, no. 12, pp. 29–39.

Aleshin, E. and Roy, R., Crystal Chemistry of Pyrochlore, *J. Am. Ceram. Soc.*, 1962, vol. 45, no. 1, pp. 18–25.

Begg, B.D., Hess, N.J., McCready, D.E., *et al.*, Heavy Ion Irradiation Effects in $Gd_2(Ti_{2-x}Zr_x)O_7$ Pyrochlores, *J. Nucl. Materials*, 2001, no. 289, pp. 188–193.

Begg, B.D., Vance, E.R., and Lumpkin, G.R., Charge Compensation and the Incorporation of Cerium in Zirconolite and Perovskite, *Proc. Symp. "Sci. Bas. Nucl. Waste Managem.-XXI,"* Warrendale: MRS, 1998, vol. 506, pp. 79–86.

Begg, B.D., Vance, E.R., Day, R.A., *et al.*, Plutonium and Neptunium Incorporation in Zirconolite, *Proc. Symp. "Sci. Bas. Nucl. Waste Managem.-XX,"* Pittsburgh: MRS, 1997, vol. 465, pp. 325–333.

Belov, N.V., Essays in Structural Mineralogy, *Mineral. sb. L'vov. Geol. O–va*, 1950, no. 4, pp. 21–34.

Burakov, B.E. and Anderson, E.B., Development of Plutonium Ceramics in Radium Institute, *Obzor dogovorov s LLNL po obrashcheniyu s izbytochnym plutoniem v Rossii. Livermorskaya nats. lab. im. Lourensa. UCRL-ID-149341* (Review of Contracts with LLNL on the Usage of Excessive Plutonium in Russia, Lourence Livermore National Laboratory. UCRL-ID-149341), Livermore: LLNL, 2002, pp. 264–269.

Burakov, B.E., Anderson, E.B., Knecht, D.A., *et al.*, Synthesis of Garnet/Perovskite-Based Ceramics for the Immobilization of Pu-Residue Wastes, *Proc. of Symp. "Sci. Bas. Nucl. Waste Managem.-XXII,"* Warrendale: MRS, 1999, vol. 556, pp. 55–62.

Burakov, B.E., Anderson, E.B., Zamoryanskaya, M.V., and Petrova, M.A., Synthesis and Study of $^{239}$Pu-Doped Gadolinium-Aluminum Garnet, *Proc. Symp. "Sci. Bas. Nucl. Waste Managem.-XXIII,"* Warrendale: MRS, 2000, vol. 608, pp. 419–422.

Chakoumakos, B.C., Systematic of the Pyrochlore Structure Type, Ideally $A_2B_2X_6Y$, *J. Solid State Chem.*, 1984, vol. 53, pp. 120–129.

Chakoumakos, B.C. and Ewing, R.C., Crystal Chemical Constraints on the Formation of Actinide Pyrochlores, *Proc. Symp. "Sci. Bas. Nucl. Waste Managem. VIII,"* Pittsburgh: MRS, 1985, vol. 44, pp. 641–646.

*Diagrammy sostoyaniya sistem tugoplavkikh oksidov* (Phase Diagrams of Systems of High-Melting Oxides), Galakhov, F.Ya., Ed., Leningrad: Nauka, 1985.

Deer, W., Howie, R., and Zusman, G., *Rock-Forming Minerals*, London: Longmans, 1962, 1963, vol. 1. Translated under the title *Porodoobrazuyushchie mineraly*, Moscow: Mir, 1965, vol. 1.

Dowty, E., Crystal Chemistry of Titanian and Zirconian Garnets: 1. Review and Spectral Studeis, *Am. Mineral.*, 1971, vol. 56, nos. 11–12, pp. 1983–2009.

Ebbinghaus, B.B., Van Konynenburg, R.A., Ryerson, F.J., *et al.*, Ceramic Formulation for the Immobilization of Plutonium, *Proc. Int. Conf. Waste Management'98. Tucson, Arizona, USA. 1-5/03/*, 1998, CD version.

Ewing, R.C., Nuclear Waste Forms for Actinides, *Proc. Natl. Acad. Sci. USA*, 1999, vol. 96, pp. 3432–3439.

Fielding, P.E. and White, T.J., Crystal-Chemical Incorporation of High Level Waste Sepcies in Aluminotitanate-Based Ceramics: Valence, Location, Radiation Damage, and Hydrothermal Durability, *J. Mater. Res.*, 1987, vol. 2, no. 3, pp. 387–414.

Flowers, R.H., Roberts, L.E.J., and Tymons, B.J., Characteristics and Quantities of Radioactive Wastes, *Phil. Trans. Royal Society Lond.*, 1986, vol. A319, pp. 5–16.

Fursenko, B.A., Synthesis of New Chrom-Bearing Garnets at High Pressure, *Dokl. Akad. Nauk SSSR*, 1980, vol. 250, no. 4, pp. 945–949.

Fursenko, B.A., Synthesis of New Silicate Garnets of High Pressure: $Mn_3M_2Si_3O_{12}$ ($M$ = V, Mn, Ga), *Dokl. Akad. Nauk SSSR*, 1983, vol. 268, no. 2, pp. 421–424.

Geller, S., Crystal Chemistry of the Garnets, *Zeits. für Kristallogr.*, 1967, vol. 125, pp. 1–47.

Geller, S. and Miller, C.E., Silicate Garnet–Yttrium-Iron Garnet Solid Solution, *Am. Mineral.*, 1959, vol. 44, nos. 11–12, pp. 1115–1120.

Gentile, A.L. and Roy, R., Isomorphism and Crystalline Solubility in the Garnet Family, *Am. Mineral.*, 1960, vol. 45, nos. 5–6, pp. 701–711.

*Glass as a Waste Form and Vitrification Technology*, Washington: Natl. Acad. Press, 1996.

Grachev, A.F., Skiba, O.V., Bychkov, A.V., *et al.*, An Experience of Conversion of Russian Plutonium of Gun's Origin and Nuclear Fuel of High-Velocity Reactors, *Obzor dogovorov s LLNL po obrashcheniyu s izbytochnym plutoniem v Rossii. Livermorskaya nats. lab. im. Lourensa* (Review of Contracts with LLNL on the Usage of Excessive Plutonium in Russia, Lourence Livermore National Laboratory, UCRL-ID-149341), Livermore: 2002, pp. 168–190.

Hench, L.L., Clark, D.E., and Campbell, J., High Level Waste Immobilization Forms, *Nucl. Chem. Waste Management*, 1984, vol. 5, pp. 149–173.

Isupov, V.A., Geometric Criterion of the Pyrochlor-Type Structure, *Kristallografiya*, 1958, vol. 3, no. 1, pp. 99–100.

Ito, J. and Frondel, C., Synthesis Zirconium and Titanium Garnets, *Am. Mineral.*, 1967, vol. 52, nos. 5–6, pp. 773–781.

Jaffe, H., The Role of Yttrium and Other Minor Elements in the Garnet Group, *Am. Mineral.*, 1951, vol. 36, nos. 1–2, pp. 133–155.

Kotova, N.P., Thermodynamic and Experimental Study of Stability of Na-Alumophosphate Glass in Connection with the Problem of Deep-Level Radioactive Waste Disposal, *Extended Abstract of Cand. Sci. (Chem.) Dissertation*, Moscow: GEOKhI, 2001.

Laverov, N.P., Omel'yanenko, B.I., Yudintsev, S.V., Nikonov, B.I., Sobolev, I.A., and Stefanovskii, S.V., Mineralogy and Geochemistry of Conserving Matrices of Radioactive Wastes, *Geol. Rudn. Mestorozhd.*, 1997, vol. 39, no. 3, pp. 211–228.

Laverov, N.P., Yudintsev, S.V., Stefanovskii, S.V., and Dzhang, Ya.N., On New Actinic Matrices with Pyrochlor Structure, *Dokl. Akad. Nauk*, 2001, vol. 381, no. 3, pp. 399–402.

Laverov, N.P., Yudintsev, S.V., Stefanovskii, S.V., Dzhang, Ya.N., Bae, I., and Che, S., Special features of Phase Formation in Synthesis of Matrices of Actinides, *Dokl. Akad. Nauk*, 2002, vol. 383, no. 1, pp. 95–98.

Lumpkin, G.R., Chakoumakos, B.C., and Ewing, R.C., Mineralogy and Radiation Effects of Microlite from the Harding Pegmatite, Taos County, New Mexico, *Am. Mineral.*, 1986, vol. 71, pp. 569–588.

Lutz, W. and Ewing, R.C., Glass and Ceramic Waste Forms–Applications and Material Properties, *Ceramic Transactions*, 1995, vol. 61, pp. 357–364.

Matyunin, Yu.I., Localization of Components of Liquid Highly Active Wastes (REE, U, and Pu) in Phosphate and Borosilicate Glass-Type Materials, *Extended Abstract of Cand. Sci. (Chem.) Dissertation*, Moscow: VNIINM, 2000.

Matzke, Hj. and van Geel, J., Incorporation of Pu and Other Actinides in Borosilicate Glass and in Waste Ceramics, *Disposal of Weapon Plutonium*, Netherlands: Kluwer, 1996, pp. 93–105.

McCauley, R.A., Structural Characteistcs of Pyrochlore Formation, *J. Appl. Phys.*, 1980, vol. 51, no. 1, pp. 290–294.

Menzer, G., Die Kristallstruktur der Granate, *Z. Kristallogr.*, 1928, vol. 69, pp. 300–396.

Mill', B.V. and Ronniger, G., Unusual Coordination Ion Numbers in the Garnet Structure, *Kristallografiya*, 1973, vol. 18, no. 1, pp. 126–132.

Mill', B.V., Belokoneva, E.L., Simonov, M.A., and Belov, N.V., Crystallochemistry of Germanium Garnets, *Problemy kristallografii* (Problems of Crystallography), Moscow: Mosk. Gos. Univ., 1982, pp. 161–179.

*Mineraly. Spravochnik* (Minerals: Handbook), Chukhrov, F.V. and Bonshtedt-Kupletskaya, E.M., Eds., Moscow: Nauka, 1967, vol. 2, no. 3.

Nikiforov, A.S., Polyakov, A.S., Borisov, G.B., *et al.*, Development of Methods for Solidification of Liquid Highly Active Wastes in the Soviet Union, *Trudy 2-i konferentsii Yadernogo O–va* (Proc. 2nd Conf. Nuclear Society), Moscow, 1992, part 2, pp. 260–266.

Nishizawa, H. and Koizumi, M., Synthesis and Infrared Spectra of $Ca_3Mn_2Si_3O_{12}$ and $Cd_3B_2Si_3O_{12}$ (B: Al, Ga, Cr, V, Fe, Mn) Garnets, *Am. Mineral.*, 1975, vol. 60, nos. 1–2, pp. 84–87.

Novak, G.A. and Gibbs, G.V., The Crystal Chemistry of the Silicate Garnets, *Am. Mineral.*, 1971, vol. 56, nos. 5–6, pp. 791–825.

*Radioactive Waste Forms for the Future*, New York: Elsevier, 1988.

Raison, P.E., Haire, R.G., Sato, T., and Ogawa, T., Fundamental and Technological Aspects of Actinide Oxide Pyrochlores: Relevance for Immobilization Matrices, *Proc. Symp. "Sci. Bas. Nucl Waste Managem.-XXII,"* Warrendale: MRS, 1999, vol. 556, pp. 3–10.

*Rentgenovskaya baza dannykh PCPDFWIN 2.02. JCPDS-ICDD* (X-ray Database PCPDFWIN 2.02. JCDPS-ICDD), 1999.

Rickwood, P.C., On Recasting Analyses of Garnet into End-Member Molecules, *Contrib. Miner. Petrol.*, 1968, vol. 18, no. 2, pp. 175–198.

Ringwood, A.E., Disposal of High-Level Nuclearwastes: A Geological Perspective, *Mineral. Mag.*, 1985, vol. 49, part 2, pp. 159–176.

Roedder, E., Formation, Handling, Storage, and Disposal of Nuclear Wastes, *J. Geol. Education*, 1990, vol. 38, no. 5, pp. 380–388.

Schingaro, E., Scordari, F., Capitanio, F., *et al.*, Crystal Chemistry of Kimzeyite from Anguillara, Mts. Sabatini, Italy, 2001, *Eur. J. Mineral.*, 2001, vol. 13, pp. 749–759.

Shannon, R.D., Revised Effective Ionic Radii and Systematic Studies of Interatomic Distance in Halides and Chalcogenides, *Acta Crystallogr.*, 1976, vol. 32, part A, pp. 751–767.

Shoup, S.S. and Bambergher, C.E., Syntheses of Titanate-Based Hosts for the Immobilization of Pu (III) and Am (III), *Proc. Symp. "Sci. Bas. Nucl. Waste Managem.-XX,"* Pittsbrugh: MRS, 1997, vol. 465, pp. 379–386.

Smelova, T.V., Krylova, N.V., Yudintsev, S.V., and Nikonov, B.S., Silicate Matrix of Actinides, *Dokl. Akad. Nauk*, 2000, vol. 374, no. 2, pp. 242–246.

Solomah, A.G., Sridhar, T.S., and Jones, S.C., Immobilization of Uranium-Rich High-Level Radioactive Liquid Waste in Synroc-FA, *Advances in Ceramics. Nucl. Waste Managem. Columbus*, Am. Ceram. Soc., 1986, vol. 20, pp. 259–265.

Sombret, G.S., Waste Forms for Conditioning High Level Radioactive Solutions, *Geol. Dist. High Level Rad. Wastes. Athens*, Teoph. Publ., 1987, pp. 69–160.

Stefanovksy, S.V., Yudintsev, S.V., Nikonov, B.S., *et al.*, Pyrochlore-Type Phases for Actinides and Rare Earths Elements Immobilization, *Proc. Symp. "Sci. Bas. Nucl. Waste Managem.-XXII,"* Warrendale: MRS, 1999, vol. 556, pp. 27–34.

Subramanian, M.A., Aravamudan, G., and Subba Rao, G.V., Oxide Pyrochlores–a Review, *Progr. Sol. State Chem.*, 1983, vol. 15, pp. 55–143.

Toropov, N.A., Barzakovskii, V.L., Lapin, V.V., and Kurtseva, N.N., *Diagrammy sostoyaniya silikatnykh sistem. Vyp. 1. Dvoinye sistemy* (Diagrams of State of Silicate Systems, issue 1: Binary Systems), Leningrad: Nauka, 1969.

Vance, E.R., Begg, B.D., Day, R.A., and Ball, C.J., Zirconolite-Rich Ceramics for Actinide Wastes, *Proc. Symp. "Sci.*

*Bas. Nucl. Waste Managem.-XVIII,"* Pittsburgh: MRS, 1995, vol. 353, pp. 767–774.

Vashman, A.A., Demin, A.V., Krylova, N.V., *et al.*, *Fosfatnye stekla s radioaktivnymi otkhodami* (Phosphate Glasses with Radioactive Wastes), Moscow: TsNIIAtominform, 1997.

Vlasov, V.I., Kedrovskii, O.L., Nikiforov, A.S., *et al.*, Manipulation of Liquid Radioactive Wastes in the Context of Conception on Closed Nuclear Fuel Cycle, *JAEA M-294/3*, Vienna, 1987, pp. 109–116.

Wang, S.X., Begg, B.D., Wang, L.M., *et al.*, Radiation Stability of Gadolinium Zirconate: A Waste Form for Plutonium Disposition, *J. Mater. Research*, 1999, vol. 14, no. 12, pp. 4470–4473.

Weber, W.J., Ewing, R.C., Catlow, C.R.A., *et al.*, Radiation Effects in Crystalline Ceramics for the Immobilization of High-Level Nuclear Waste and Plutonium, *J. Mater. Research*, 1998, vol. 13, no. 6, pp. 1434–1482.

Xu, H., Wang, Y., Putnam, R.L., *et al.*, Microstructure and Composition of Synroc Samples Crystallized from a $CaCeTi_2O_7$ Chemical System: HRETEM/EELS Investigation, *Proc. Symp. "Sci. Bas. Nucl. Waste Managem.-XXII,"* Warrendale: MRS, 2000, vol. 608, pp. 461–466.

Yudintsev, S.V., Matrices for Radioactive Waste Immobilization: Status and Prospects, *Excess Weapons Plutonium Immobilization in Russia, LLNL, UCRL-JD-138361*, 2000, pp. 275–282.

Yudintsev, S.V., Lapina, M.I., Ptashkin, A.G., *et al.*, Uranium Accommodation into Garnet Host, *Proc. Symp. "Sci. Bas. Nucl. Waste Managem.-XXV,"* Warrendale: MRS, 2002. CD-version, 2002, vol. 713, Paper JJ 11.28.